

Local Strain Distribution in Synthetic Diamond Crystals, Determined by the Parameters of the Energy Spectrum of the Kikuchi Patterns

I. M. Fodchuk^a, S. A. Ivakhnenko^b, V. N. Tkach^{b, *}, S. V. Balovsyak^a, M. D. Borcha^a,
N. S. Solodkii^a, I. I. Gutsulyak^a, A. R. Kuzmin^a, and O. V. Sumaryuk^a

^a*Fedkovych National University, Chernivtsi, 58012 Ukraine*

^b*V. Bakul Institute for Superhard Materials, National Academy of Sciences of Ukraine, Kyiv, 04074 Ukraine*

**e-mail: tkach@ism.kiev.ua*

Received March 25, 2019; revised May 31, 2019; accepted June 6, 2019

Abstract—The average strain in local regions of synthetic diamond was determined using the energy Fourier-transform spectrum in the analysis of digital Kikuchi patterns. The degree of broadening of the diffraction bands and their intersections in the images caused by deformations is quantitatively described through the average spatial period and the area of the radial distribution of the energy spectrum. The planar distribution of local strains made it possible to determine their anisotropy in the crystal in magnitude and direction.

Keywords: synthetic diamonds, Kikuchi lines, backscattered electron diffraction, Fourier transform, Fourier-transform energy spectrum

DOI: 10.3103/S1063457620010049

INTRODUCTION

Great interest in natural and synthetic diamond crystals is caused by their unique physical and chemical properties, in particular, high thermal conductivity at room temperature, hardness, wear and radiation resistance, chemical inertness, and exceptional optical and electrical characteristics (for example, high resistivity) [1, 2].

A large number of different methods are known for studying the defective system and structure of diamonds or diamond-like crystals [3–12]. In particular, to determine the degree of homogeneity and perfection of crystalline materials, the use of diffraction of backscattered electrons (the Kikuchi method) is rather promising [7–9]. In the Kikuchi method, an electron diffraction image can be recorded from individual sections of a sample, several tens of nanometers in size. This enables one to determine the crystallographic orientation of the grains, the angular misorientation between them ($<0.1^\circ$), and the strain state in individual grains [3–6]. The prospect of wider use of the Kikuchi method may be associated with the improvement of computer methods of data processing [8–10]. Some of them have already been used to obtain the average local strains in crystals, in particular, by using the two-dimensional Fourier transform of the Kikuchi patterns and by analyzing the band intensity profiles and the displacement of the axis of the zones [10–13].

In this work, we tested and used a new approach to estimate the strain in individual local regions of diamond crystals. To analyze the changes in the shape and area of the intensity profile of the Kikuchi bands, we used a discrete two-dimensional Fourier transform of the Kikuchi patterns and their Fourier-transform energy spectrum. This significantly increased the information content and unambiguity of the interpretation of changes in the profile geometry of the Kikuchi bands and, therefore, made it possible to assess changes in the fine structure of diamonds quantitatively.

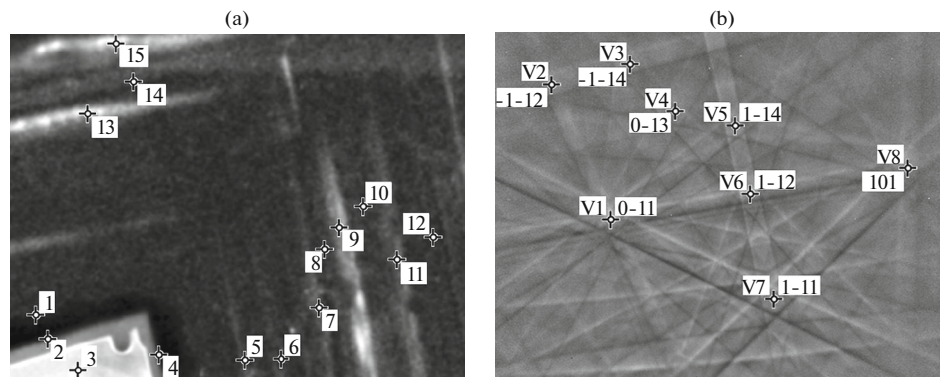


Fig. 1. Fragment of the surface of a diamond, $170 \times 120 \mu\text{m}$ in size, obtained using cathodoluminescent topography: (a) markers indicate sections 1–15 in which the Kikuchi patterns were obtained; (b) markers V1–V8 indicate the indices of the axis of the zones and the nodes between which the intensity profiles of the Kikuchi bands were determined.

EXPERIMENTAL

To determine the strain state of synthetic diamonds, studies were carried out using a Zeiss EVO 50 XVP scanning electron microscope (Carl Zeiss, Germany) equipped with a CCD detector. The angle of incidence of the electron beam on the crystal surface was 70° .

Synthetic diamonds were obtained by the temperature gradient method in the Fe–Al–C system at high (~ 6 GPa) static pressure and high (~ 1700 K) temperature; the growth time was ~ 48 h [14–16]. The surface (100) of diamond synthesized in the Ni–Mn–C system was used as a substrate.

For different sections of the test sample (indicated by numbers in Fig. 1a), the Kikuchi patterns were obtained (Fig. 1b). The position of each of the Kikuchi bands was determined using conventional software that yields information on the crystallographic orientation of the axes of zones (the region of intersection of the Kikuchi bands) [17].

We note that the Kikuchi patterns (Fig. 1b) obtained from different regions of the sample demonstrate (at a fine level) the imperfection of the structure of the diamond lattice and its structural heterogeneity in local areas.

DETERMINATION OF LOCAL STRAINS BY ANALYSING THE INTENSITY PROFILES OF KIKUCHUI BANDS

The problem of analyzing Kikuchi patterns is that the intensities of the profiles of the Kikuchi bands and the coordinates of their sections (nodes) depend not only on the structural parameters of the crystal under study but also on the experimental conditions. Depending on the experimental conditions (the angle of incidence of electrons on the sample, the distance from the sample to the electron detector, etc.), we can observe a shift in width and height of the node, compression or stretching of the image along different directions, rotation, change the average brightness, and other distortions. Therefore, to compensate for these effects, the Kikuchi patterns in sections 2–15 were aligned with a reference image in section 1 using genetic algorithms [18]. To increase the accuracy of image alignment, noise filtering was performed for the Kikuchi patterns [19, 20]. The task is to minimize the discrepancy (difference) between the image of the Kikuchi lines of the reference region of the sample and the images obtained from other regions of the crystal [19, 20].

Markers V1–V8 in Fig. 1b indicate the indices of the crystallographic axes of zones and nodes, between which the intensity profile of the Kikuchi bands was determined (Fig. 2).

The intensity of band profiles is usually normalized and analyzed when their shape changes [21]. In Fig. 2, there are differences not only in the area under the averaged profile but also in the form of intensity distributions, which indicates the presence of inhomogeneous (both in magnitude and direction) strains and, consequently, stress in the given sample of synthetic diamond.

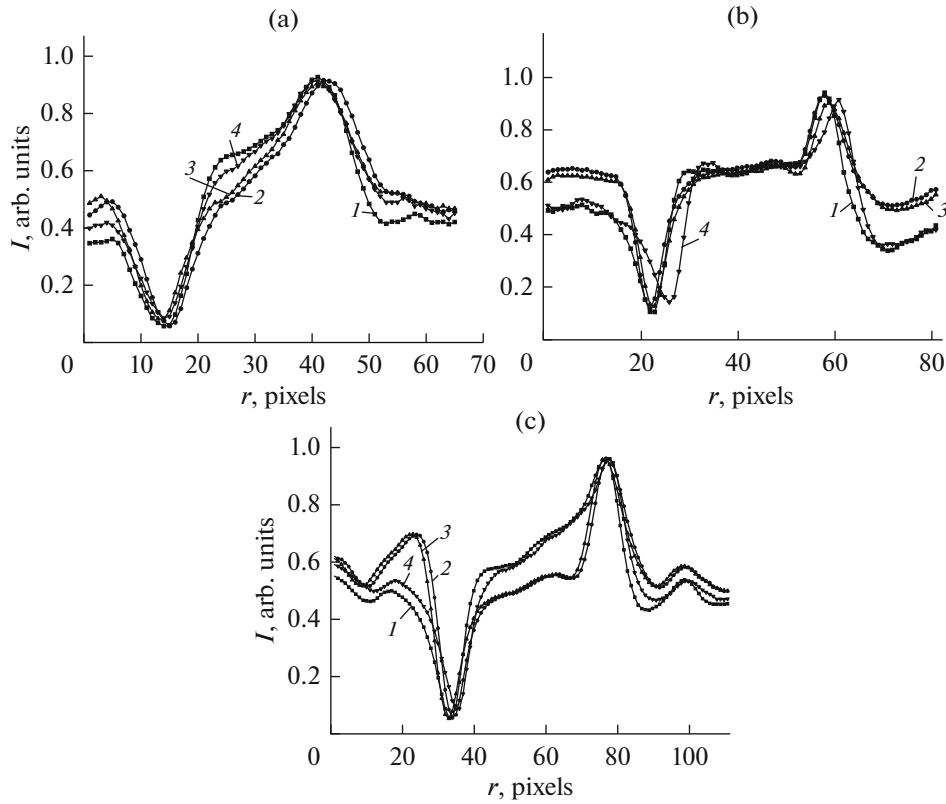


Fig. 2. Averaged profiles (*I*) p1, (2) p2, (3) p3, and (4) p4 of the intensity of the Kikuchi bands in sections 1–4 between nodes (a) V1–V2, (b) V1–V5, and (c) V1–V7 (Fig. 1b).

The local strain ε_V for a certain crystallographic direction (plane) can be calculated from the analysis of changes in the area under the intensity profile of the Kikuchi band using the relation [13],

$$\varepsilon_V = k_d \ln \left(\frac{S_{I0}}{S_I} \right), \quad (1)$$

where coefficient $k_d = 4.33 \times 10^{-3}$; S_I is the area under the profile of the band in the region with deformation; and S_{I0} is the maximum S_I value for all regions.

Figure 3 shows the distribution of strains ε_V in the local regions (n_A) of a synthetic diamond crystal, calculated using Eq. (1), and ε_S , that is, the average values of strains (ε_V^{12} , ε_V^{15} , ε_V^{17}) for all crystallographic directions.

The strains ε_V obtained for different crystallographic directions correlate well with each other (Fig. 3). A regularity is revealed in the dependence of the average values of strains $\bar{\varepsilon}_V$ (for all regions of the crystal) on the crystallographic direction: the minimum value is $\bar{\varepsilon}_V^{15} = 0.1255 \times 10^{-3}$ for the direction $[\bar{5}\bar{1}1]$ and $\bar{\varepsilon}_V^{12} = 0.1837 \times 10^{-3}$ for $[\bar{3}1\bar{1}]$; the maximum value is $\bar{\varepsilon}_V^{17} = 0.2443 \times 10^{-3}$ for $[\bar{2}\bar{1}1]$. The detected dependence of the strain on the crystallographic direction indicates a significant anisotropy of the strains for the studied diamond crystals.

Characteristic oscillations with maxima for sections 5, 7, and 9 and minima for sections 4, 6, 8, and 10 were also found for the strains ε_S (Fig. 3). The maxima of such oscillations correspond to Fig. 1a (the bright sections 5, 7, and 9) and indicate the periodicity in the change in the structural properties of the crystals.

Based on the obtained strains ε_S , the planar distribution of strains for the studied diamond crystal was calculated by approximation (Fig. 4). The planar distribution of strains also confirms the periodicity in the change in the structural properties of crystals, especially for local maxima in sections 5, 7, and 9.

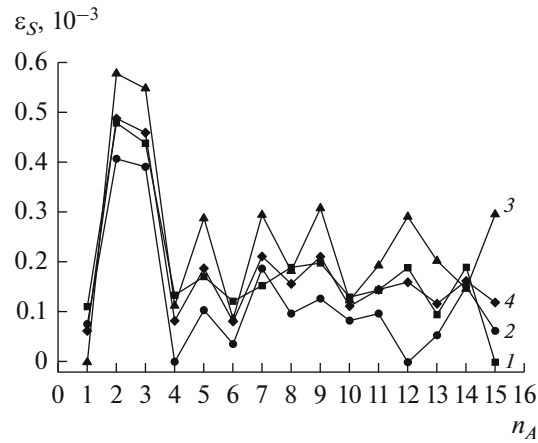


Fig. 3. Anisotropy in the distribution of strains $\varepsilon(n_A)$ in directions (Fig. 1b) of the strains calculated based on the profiles of the Kikuchi band (1) between nodes V1–V2 $[\bar{3}1\bar{1}]$, ε_V^{12} ; (2) between nodes V1–V5 $[\bar{5}\bar{1}\bar{1}]$, ε_V^{15} ; and (3) between nodes V1–V7 $[\bar{2}\bar{1}\bar{1}]$, ε_V^{17} . (4) Average strain value for all directions, ε_S .

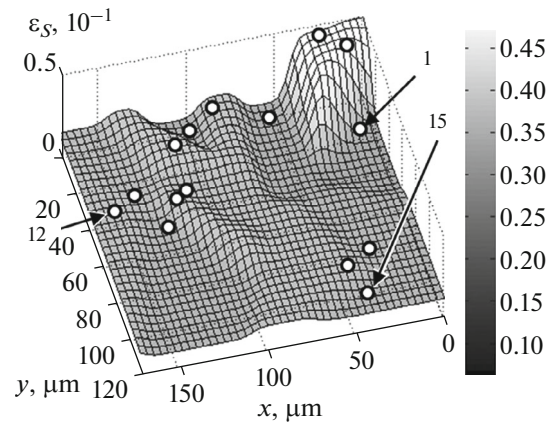


Fig. 4. Planar distribution of the ε_S strain in the local regions 1–15 of the synthetic diamond crystal (Fig. 1a).

An analysis of the features of the distribution of local strains in the crystal regions marked in Figs. 3 and 4 gives a qualitative idea not only of the nature of their anisotropy but also of the heterogeneity of the crystal growth conditions and the distribution of dopants [15, 16].

ANALYSIS OF KIKUCHI PATTERNS USING THE PARAMETERS OF THE FOURIER-TRANSFORM ENERGY SPECTRUM

The degree of broadening of the bands in the Kikuchi patterns, obtained from different sections of the crystal, varies significantly; therefore, a quantitative assessment is based on analyzing their Fourier-transform energy spectra. Image processing is performed in the MatLab software environment [22, 23].

The Fourier spectrum F of the digital image of the Kikuchi bands f was calculated using the two-dimensional discrete fast Fourier transform according to the relation [14]

$$F(m, n) = \sum_{i=0}^M \sum_{k=0}^N f(i, k) \exp\left(-2\pi j \left(\frac{m(i-1)}{M} + \frac{n(k-1)}{N}\right)\right), \quad (2)$$

where m and n are the numbers of the spectrum frequencies in height and width, respectively; $m = 1, 2, \dots, M$; $n = 1, 2, \dots, N$; M and N are the sizes of image f in pixels; and j is the imaginary unit.

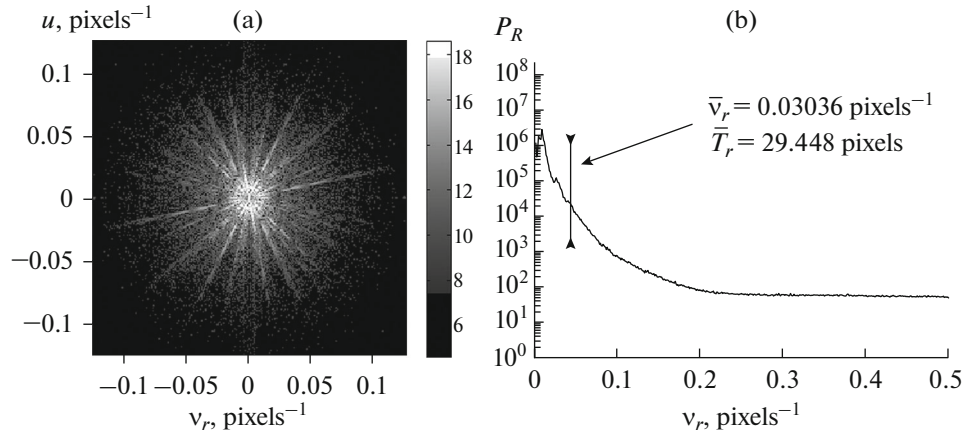


Fig. 5. (a) Energy spectrum P_S of the image of the Kikuchi bands and (b) its radial distribution P_R in a logarithmic scale; \bar{T}_r is the average radial spatial period of the image for section 1.

The energy spectrum P_S of image f is the square of the module of the centered Fourier-transform spectrum F_C , that is,

$$P_S = |F_C|^2. \quad (3)$$

For further processing, the energy spectra P_S of the Kikuchi patterns are presented in a logarithmic scale as

$$P_{SL} = \ln(C_L + P_S), \quad (4)$$

where C_L is a constant by which contrast and color gamut can be adjusted during visualization (by default, $C_L = 1$).

Logarithmic scaling enables efficient processing of the components of the P_{SL} spectrum even with a small amplitude. The obtained P_S energy spectra substantially depend on the degree of broadening of the Kikuchi bands, and, accordingly, on the value ε of local strains. To determine ε , we used the frequency characteristics of images, which depend only on the parameters of the studied objects [14].

By linear interpolation of the energy spectrum P_S , we calculated its radial distribution $P_R(d)$, where d is integer values of the distance from the spectrum element (m, n) to its center (M_C, N_C) ; $d = 1, \dots, N_R$; $N_R = N_{\min}/2$; $N_{\min} = \min(M, N)$ is the minimum size of image f . The values of $P_R(d)$ are the arithmetic mean $P_S(m, n)$ for discrete values of d . Each value of the distance d corresponds to the value of the spatial radial frequency v_r .

The obtained P_S spectra and their distribution $P_R(v_r)$ have a characteristic shape for each studied region (Fig. 5). The P_R distributions, as well as the P_S spectra, contain information on the value of ε in the studied local regions.

As a rule, the Kikuchi experimental patterns exhibit significant high-frequency noise, which appears in the P_R distributions as a background, especially at high spatial frequencies $v_r > 0.2$ pixel⁻¹. Such a noise component of the P_R distributions leads to a distortion of the mean spatial radial frequency \bar{v}_r (Fig. 5).

Therefore, to clarify the average frequency \bar{v}_r , the noise component of P_R is removed. An additive white Gaussian noise was used as a noise model [19, 22]. The level of Gaussian noise is described by its mean square deviation σ_{NE} .

The average spatial frequency \bar{v}_r of image f is calculated based on the radial distribution $P_R(d)$, where $d = 1, \dots, N_R$, without taking into account the constant component (zero frequency with number $d = 1$) according to the equation

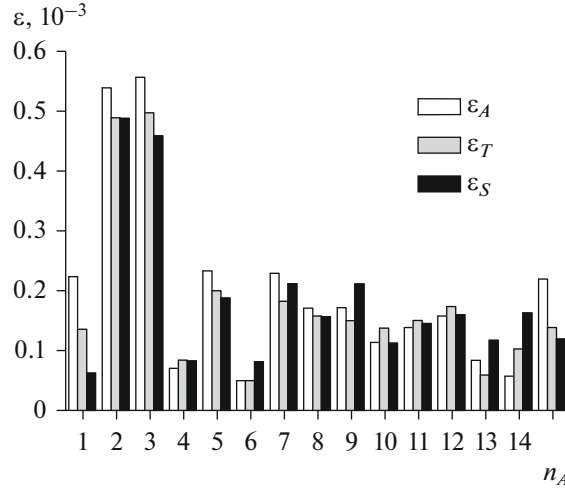


Fig. 6. Diagram of mean strain values in local regions of the diamond, calculated by various methods: strains calculated based on the radial distribution P_R area (ε_A) and average radial period \bar{T}_r (ε_T); average strains calculated based on the Kikuchi ϕ band profiles (ε_S).

$$\bar{\nu}_r = \frac{\sum_{d=2}^{N_R} P_R(d) \nu_r(d)}{\sum_{d=2}^{N_R} P_R(d)}. \quad (5)$$

The average radial spatial frequency $\bar{\nu}_r$ corresponds to the average radial spatial period

$$\bar{T}_r = \frac{1}{\bar{\nu}_r}, \quad (6)$$

which is calculated based on the radial distribution P_R in the range from T_r^{\min} to T_r^{\max} , where $T_r^{\min} = 25$ pixels and $T_r^{\max} = 75$ pixels. The minimum period value T_r^{\min} is determined as the average half-width of the Kikuchi bands, since the band profiles have clear minimums and maximums (smaller spatial periods correspond to the noise component). The maximum period value $T_r^{\max} = 75$ pixels is three middle half-widths of the bands. The spatial periods smaller than T_r^{\min} correspond to the noise component. Periods that are larger than T_r^{\max} describe primarily the background of the images rather than the brightness distribution of the Kikuchi band.

The strain of crystals $\Delta d/d$ can be determined by changing the periods ε_T and the area ε_A of the radial distributions P_R of their energy spectra according to the relations [13]

$$\varepsilon_T = k_T \ln \left(\frac{\bar{T}_r}{\bar{T}_{r0}} \right), \quad (7)$$

$$\varepsilon_A = k_A \ln \left(\frac{S_P}{S_{PM}} \right), \quad (8)$$

where coefficient $k_T = 4.33 \times 10^{-3}$ (as in the determination of strains ε_S , see Eq. (1)), $k_A = 1.4 \times 10^{-3}$ (selected by minimizing the mean square difference between ε_A and ε_S); \bar{T}_r is the average radial spatial period for the crystal region (for example, regions 1–15 in Fig. 1a); \bar{T}_{r0} is the maximum value for all sections; S_P is the distribution area of P_R for each local section (for example, sections 1–15 in Fig. 1a); and S_{PM} is the minimum S_P value for all sections.

Figure 6 shows the average strain values in each section of the sample. The resulting strains ε_T and ε_A are consistent with the strains ε_S calculated based on the band profiles.

To accord the results of determining the strain ε_S of the crystals based on the intensity profiles of the Kikuchi bands, a constant component $\Delta\varepsilon = 0.5 \times 10^{-4}$ is added to the values of ε_T and ε_A .

The insignificant difference between the values of ε_T , ε_A , and ε_S can be explained by different approaches to their determination. The strain value ε_S depends on the individual components of the strain tensor and is associated with the crystallographic orientation of the bands. The consistency between the values of ε_T , ε_A , and ε_S indicates the prospect of using the Fourier-transform energy spectrum for the analysis of the Kikuchi patterns.

CONCLUSIONS

The use of the Fourier-transform energy spectra in addition to the method of discrete two-dimensional Fourier transform of backscattered electron diffraction patterns has created additional possibilities for determining the average strain values in local regions of synthetic diamonds. This improved the information content and unambiguity of the interpretation of changes in the geometry of the Kikuchi bands.

The Kikuchi experimental patterns from different regions of the same sample are characterized by varying degrees of broadening of the diffraction bands. The degree of broadening of the bands in the Kikuchi patterns is associated with strains ε_T and ε_A , which can be quantitatively described through the average spatial period and the area of the radial distribution of the energy spectrum of the Kikuchi pattern.

Aligning the Kikuchi patterns using genetic algorithms and filtering white Gaussian noise to analyze the obtained Kikuchi patterns with varying degrees of broadening enable taking into account the effect of instrumental factors on the formation of backscattered electron diffraction patterns.

An analysis of the characteristics of the distribution of average strains in local regions of the crystal on planar distributions gives not only a qualitative idea of the nature of their anisotropy but also a qualitative idea of the possible nature of the effect of technological parameters on the inhomogeneity of crystal growth conditions.

REFERENCES

1. Chalker, P.R., Johnston, C., and Werner, M., Physical properties of diamond for thermistors and pressure transducers, *Semicond. Sci. Technol.*, 2003, vol. 18, no. 3, pp. S113–S116.
2. *Fizicheskie svoystva almaza: Spravochnik* (Physical Properties of Diamond: Handbook), Novikov, N.V., Ed., Kiev: Naukova Dumka, 1987.
3. *Electron Backscatter Diffraction in Materials Science*, Schwartz, A.J., Kumar, M., Adams, B.L., and Field, D.P., Eds., Berlin: Springer-Verlag, 2009.
4. Kaboli, S. and Burnley, P.C., Direct observations of crystal defects in polycrystalline diamond, *Mater. Charact.*, 2018, vol. 142, pp. 154–161.
5. Fodchuk, I., Balovsyak, S., Borcha, M., Garabazhiv, Ya., and Tkach, V., Determination of structural inhomogeneity of synthesized diamonds by backscattering electron diffraction, *Phys. Status Solidi A*, 2011, vol. 208, no. 11, pp. 2591–2596.
6. Hagihara, K., Okamoto, T., Yamasaki, M., Kawamura, Y., and Nakano, T., Electron backscatter diffraction pattern analysis of the deformation band formed in the Mg-based long-period stacking ordered phase, *Scr. Mater.*, 2016, vol. 117, pp. 32–36.
7. Vilalta-Clemente, A., Naresh-Kumar, G., Nouf-Allahiani, M., Gamarra, P., di Forte-Poisson, M.A., Trager-Cowan, C., and Wilkinson, A.J., Cross-correlation based high resolution electron backscatter diffraction and electron channeling contrast imaging for strain mapping and dislocation distributions in InAlN thin films, *Acta Mater.*, 2017, vol. 125, pp. 125–135.
8. Dingley, D.J., Wilkinson, A.J., Meaden, G., and Karamched, P.S., Elastic strain tensor measurement using electron backscatter diffraction in the SEM, *J. Electron. Microsc.*, 2010, vol. 59, suppl. 1, pp. S155–S163.
9. Stoll, A. and Wilkinson, A.J., Simulation of deformation twins and their interactions with cracks, *Comput. Mater. Sci.*, 2014, vol. 89, pp. 224–232.
10. Sasaki, Y., Igushi, M., and Hino, M., Measuring strains for hematite phase in sinter ore by electron backscattering diffraction method, *Key Eng. Mater.*, 2006, vols. 326–328, pp. 237–240.
11. Borcha, M.D., Balovsyak, S.V., Fodchuk, I.M., Khomenko, V.Yu., and Tkach, V.N., Distribution of local deformations in diamond crystals according to the analysis of Kikuchi lines profile intensities, *J. Superhard Mater.*, 2013, vol. 35, no. 4, pp. 220–226.

12. Borcha, M.D., Balovsyak, S.V., Fodchuk, I.M., Khomenko, V.Yu., Kroitor, O.P., and Tkach, V.N., A strain state in synthetic diamond crystals by the data of electron backscatter diffraction method, *J. Superhard Mater.*, 2016, vol. 38, no. 4, pp. 271–276.
13. Wright, S. I., Nowell, M. M., and Field, D.P., A review of strain analysis using electron backscatter diffraction, *Microsc. Microanal.*, 2011, vol. 17, no. 3, pp. 316–329.
14. Borcha, M.D., Balovsyak, S.V., Fodchuk, I.M., Khomenko, V.Yu., Kroitor, O.P., and Tkach, V.N., Local deformation in diamond crystals defined by the Fourier transformations of Kikuchi patterns, *J. Superhard Mater.*, 2013, vol. 35, no. 5, pp. 284–291.
15. Novikov, N.V., Nachalna, T.A., Ivakhnenko, S.A., Zanevsky, O.A., Belousov, I.S., Malogolovets, V.G., Podz'yarei, G.A., and Romanko, L.A., Properties of semiconducting diamonds grown by the temperature-gradient method, *Diamond Relat. Mater.*, 2003, vol. 12, nos. 10–11, pp. 1990–1994.
16. Lysakovskii, V.V., Ivakhnenko, S.A., and Katrusha, A.N., Effect of the titanium doping of the Fe–Co–C solvent on the nitrogen content of diamond single crystals grown at high pressures and temperatures, *J. Superhard Mater.*, 2007, vol. 29, no. 6, pp. 38–44.
17. Wilkinson, A. and Britton, B., Strains, planes, and EBSD in materials science, *Mater. Today*, 2012, vol. 15, no. 9, pp. 366–376.
18. Balovsyak, S.V. and Fodchuk, I.M., Objects images alignment with the use of genetic and gradient algorithms, *Int. J. Comput.*, 2013, vol. 12, no. 2, pp. 160–167.
19. Balovsyak, S.V. and Odaiska, Kh.S., Automatic highly accurate estimation of Gaussian noise level in digital images using filtration and edges detection methods, *Int. J. Image, Graphics Signal Process.*, 2017, vol. 9, no. 12, pp. 1–11.
20. Balovsyak, S.V. and Odaiskaya, Kh.S., Automatic determination of level of Gaussian noise in digital images by method of the selected regions, *Kibern. Vychisl. Tekh. (Kiev)*, 2017, vol. 3, no. 189, pp. 43–60.
21. Borcha, M.D., Zvyagintseva, A.V., Tkach, V.N., Yushchenko, K.A., Balovsyak, S.V., Fodchuk, I.M., and Khomenko, V.Yu., Local deformations in near crack of nickel-alloy weld seam determined by the Fourier transformation of Kikuchi paintings, *Metallofiz. Noveishie Tekhnol.*, 2013, vol. 35, no. 10, pp. 1359–1370.
22. Gonzalez, R.C. and Woods, R.E., *Digital Image Processing*, New Jersey: Prentice Hall, 2001.
23. Gonzalez, R.C., Woods, R.E., and Eddins, S.L., *Digital Image Processing Using MATLAB*, New Delhi: Pearson Education, 2004.

Translated by O. Zhukova